

## Very fast photometric observations of the intermediate polar V2069 Cygni

---

**Ilham Nasiroglu\***

*Max Planck Institute for Extraterrestrial Physics, Giessenbachstrasse 1, 85741 Garching, Germany*

*Department of Physics, University of Cukurova, 01330 Adana, Turkey*

*E-mail: ilhamnasiroglu@yahoo.com*

**Agnieszka Słowikowska**

*Institute of Astronomy, University of Zielona Góra, Lubuska 2, 65-265 Zielona Góra, Poland*

*E-mail: aga@astro.ia.uz.zgora.pl*

**Gottfried Kanbach**

*Max Planck Institute for Extraterrestrial Physics, Giessenbachstrasse 1, 85741 Garching, Germany*

*E-mail: gok@mpe.mpg.de*

We present fast timing photometric observations of the intermediate polar V2069 Cygni (RX J2123.7+4217) using the Optical Timing Analyzer (OPTIMA) at the Skinakas Observatory 1.3 m telescope. OPTIMA is a single-photon counting aperture photo-polarimeter with the timing accuracy of about 4 microseconds and absolute (GPS) tagging of photon arrival-times. The optical (450-950 nm) light curve of V2069 Cygni was measured with sub-second resolution during July 2009 and revealed a double-peaked pulsation with 743.385 ( $\pm 0.250$ ) s period. A similar double-peaked modulation was found in simultaneous soft X-ray observations with the Swift satellite. We suggest that the 743.385 ( $\pm 0.250$ ) s period represents the spin of the white dwarf accretor. In the  $P_{\text{orb}}-P_{\text{spin}}$  diagram of all IPs, V2069 Cyg is rather an indistinct member of this population. It has however a rather low spin to orbit ratio of  $\sim 0.027$ .

*High Time Resolution Astrophysics (HTRA) IV - The Era of Extremely Large Telescopes*

*May 5 - 7, 2010*

*Agios Nikolaos, Crete Greece*

---

\*Speaker.

## 1. Introduction

Magnetic cataclysmic variables (CVs) are interacting close binary systems in which material transferred from a Roche-lobe filling low mass companion is accreted by a magnetic white dwarf (WD). Magnetic CVs are subdivided in two groups: polars (or AM Her type) and intermediate polars (IPs; or DQ Herculis type). In polars, the WD has a sufficiently strong magnetic field ( $B \sim 10^7 - 10^8$  G) which locks the system into synchronous rotation ( $P_{\text{spin}} = P_{\text{orb}}$ ) and prevents the accretion disk to form around the WD. In IPs, the field of the WD is slightly weaker ( $B \sim 10^6 - 10^7$  G) which does not force the WD to spin with the same period as the binary system ( $P_{\text{spin}} < P_{\text{orb}}$ ). The accretion in IPs happens through a disk with a disrupted inner region [1, 2, 3, 4].

V2069 Cyg (RX J2123.7+4217) was discovered as a hard X-ray source by Motch et al. (1996) and identified as a CV [5]. Thorstensen and Taylor (2001) reported a most probable orbital period of 0.311683 days from spectroscopic observations [6]. De Martino et al. (2009) performed a preliminary analysis of XMM-Newton observations that showed strong peaks at the fundamental frequency of 116.3 cycles/day and harmonics up to the third [7]. The sinusoidal fit to the profile from both EPIC-pn and MOS data revealed a fundamental period of  $743.2 \pm 0.4$  s and 55% pulse fraction. The spectral analysis confirmed that V2069 Cyg is a hard X-ray emitting IP with a soft X-ray component.

## 2. Observations

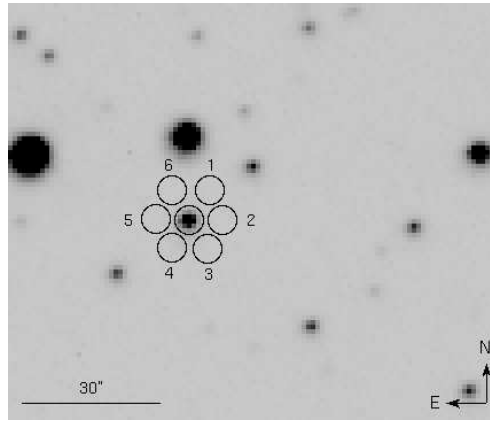
We performed photometric observations of V2069 Cyg with the Optical Timing Analyzer (OPTIMA) instrument at Skinakas Observatory, Crete, Greece and simultaneous soft X-ray observations with the Swift/X-ray telescope (XRT) in the energy range of 0.3-10 keV. Swift XRT operated in Photon-Counting mode with a time resolution of 2.5073 s. The log of the observations is given in Tab. 1. The high-speed photometer OPTIMA has been designed as a sensitive, portable detector to observe extremely faint optical pulsars and other highly variable astrophysical sources. The detector contains eight fiber-fed single photon counters - avalanche photodiodes (APDs), and a GPS for the time control. The fiber array is configured as a hexagonal bundle (Fig. 1). A separate fiber is located at a distance of  $\sim 1'$  as a night sky background monitor. Single photons are recorded in all channels with absolute timing accuracy of  $\sim 4\mu\text{s}$ . The quantum efficiency of APDs reaches a maximum of 60% at 750nm and lies above 20% in the range 450-950nm [8].

## 3. Data analysis

We analysed the data using the HEASoft analysis package, *FTOOLS* ver. 6.9 and *XRONOS* ver. 5.22. The source position obtained from Swift data is: RA (J2000) = 21 23 44.69, Dec (J2000) = +42 17 59.6 with an error radius of 3.5 arcseconds. OPTIMA was pointed at RA (J2000) = 21 23 44.82, Dec (J2000) = +42 18 01.7. The X-ray and optical photon arrival times were converted to the solar system barycentric time. For XRT data we applied the following types of filters: grade 0-4, energy 0.3-10 keV and a circle region filter centered at the position of the source with 10 pixels radius (corresponding to  $\sim 23.5$  arcsec). OPTIMA count rates of the source were obtained from the central fiber (Fig. 1). Raw data were binned with 1 s and the corresponding background counts were subtracted. The fiber number 5 was chosen as the best representative of the background (Fig. 2).

**Table 1:** Log of the photometric (OPTIMA) and X-ray (*Swift*) observations of V2069 Cyg

No.	Date 2009	Detector	ObsBeg (MJD)	Expo. (h)
1	Jul 02	OPTIMA	55014.922	2.5
2	Jul 18	OPTIMA	55030.951	1.2
3	Jul 19	OPTIMA	55031.845	2.1
4	Jul 21	OPTIMA	55033.820	4.1
5	Jul 22	OPTIMA	55034.871	3.0
6	Jul 24	OPTIMA	55036.804	1.2
7	Jul 26	OPTIMA	55038.040	1.4
8	Jul 26	OPTIMA	55038.827	1.7
9	Jul 28	OPTIMA	55040.897	1.5
A	Jul 21	<i>Swift</i>	55033.786	0.8
B	Jul 22	<i>Swift</i>	55034.048	0.9

**Figure 1:** OPTIMA fiber bundle centered on V2069 Cyg. The ring fibers (1-6) can be used to monitor the background sky simultaneously.

The resulting light curve shows a prominent periodic variability (Fig. 3). The power spectrum was computed with the FFT algorithm and normalized such that the white noise level expected from the data uncertainties corresponds to a power of 2 (Fig. 4). It shows peaks at the spin frequency 0.00134277 Hz and its first harmonic 0.00268555 Hz (periods 744.7 s and 372.35 s, respectively), as well as an instrumental frequency of 0.03718 (26.9 s). The 744.7-s period in the Xronos/*efsearch* task which folds the light curve with a large number of trial periods around an approximate period, reveals the best spin period of the white dwarf as 743.385 ( $\pm 0.250$ )s (Fig. 5). We found that the first harmonic is much stronger than the fundamental. Very similar behavior has been observed in the XMM-Newton data for another IP, V405 Aur. Here the first harmonic is stronger at energies below 0.7 keV, while the fundamental is stronger at energies above 0.7 keV [9].

The optical light curve folded with the 743.385-s spin period shows a double peaked profile

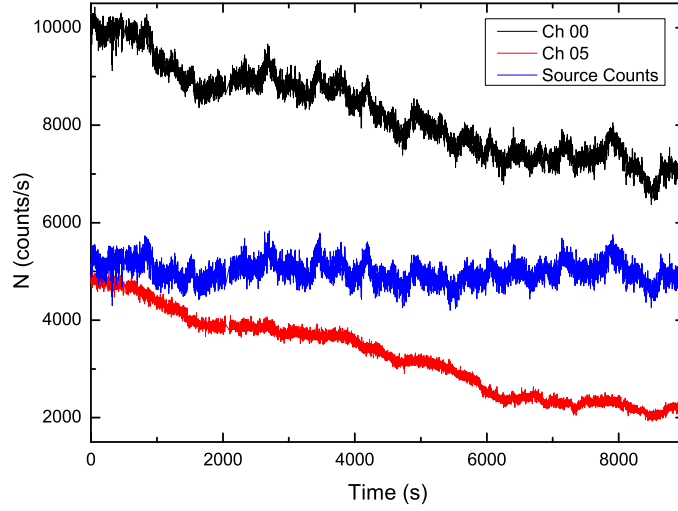


**Figure 2:** Count rates of V2069 Cyg (Tab. 1, obs. 1: July, 2009). Source count rates obtained from the central fiber (Ch 0). Raw data are binned with one second time intervals and then the corresponding background counts (Ch 5) are subtracted. The sky background is decreasing in brightness because of the setting Moon.

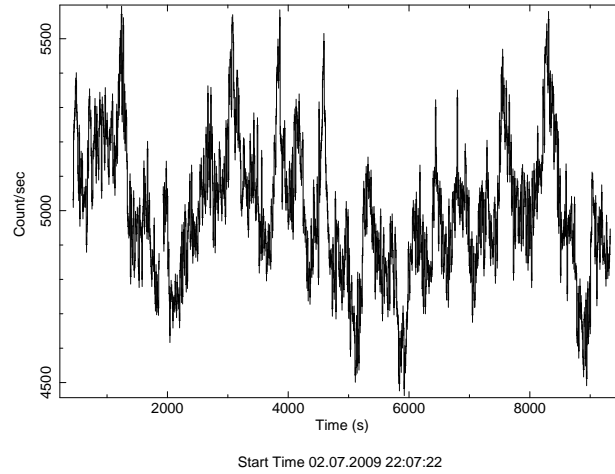


**Figure 3:** Light-curve of V2069 Cyg as derived in Fig. 2, zoomed in the countrate scale for better visibility. The optical periodicity is clearly visible.

(see Fig. 6) with very high duty cycle (90%). Its soft X-ray emission also shows a double-peak modulation at the white dwarf spin period (see Fig. 7), however the weaker peak is marginal. The optical and the X-ray light curves are out of phase. The hard emission reported by de Martino et al. (2009) has a sinusoidal modulation with 55% pulsed fraction [7]. They also reported that the X-ray pulses are anti-phased with the optical ones. If the case of V2069 Cyg is similar to that of the V405 Aur, then the optical peak that is observed with the XMM-Newton OM in the B-band most likely corresponds to the first peak in our folded OPTIMA light curve. The X-ray spectra of V2069 Cyg and V405 Aur show blackbody components with temperatures of 56 eV and 39.7 eV,

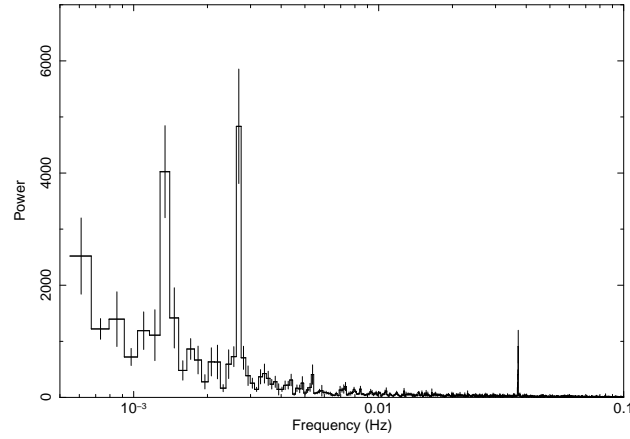


**Figure 4:** Power spectrum (all epochs) of the V2069 Cyg optical data. It shows prominent peaks at the spin frequency (0.00134277 Hz) and its first harmonic (0.00268555 Hz). An instrumental frequency at 0.0371094 Hz is also well visible.

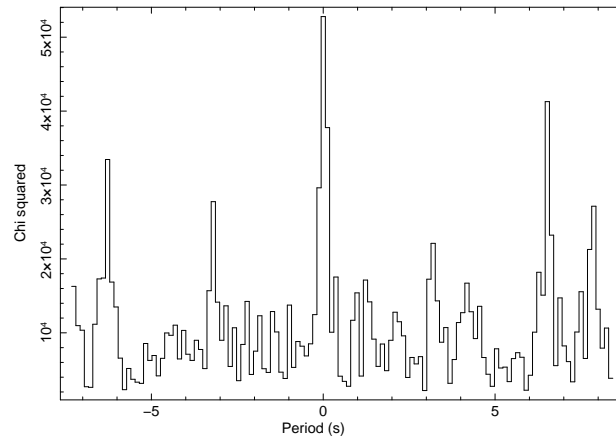


**Figure 5:**  $\chi^2$  plot as a function of trial period for OPTIMA data. The central value ( $=0$ ) corresponds to a period of 743.385 s.

respectively. Moreover, they have quite similar spin-orbit period ratios of 0.0276 for V2069 Cyg (743.385-s/26928-s) and 0.036 for V405 Aur (545.5-s/14986-s).

Most likely the modulation of the blackbody emission is due to the changing perspective onto the accreting pole caps. We view the heated surface most favorably when one of the poles points towards us, therefore we see a double-peaked modulation. The peak separation is 0.5 in phase, however the magnetic axis can not be very highly inclined (i.e. close to 90 degrees), because we see only a small difference in the peak intensities. Evans and Hellier (2004) suggested that IPs with shorter spin periods will have smaller magnetospheres in which the accretion discs are disrupted nearer to the white dwarf. This could result in shorter, fatter 'accretion curtains' of

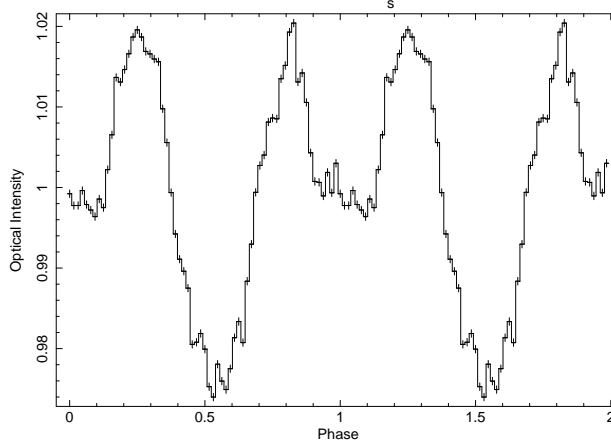


**Figure 6:** The optical data (all epochs) of V2069 Cyg folded with the 743.384825 s spin cycle (64 bins/period). Reference time  $T_0 = 55014.000$  MJD.

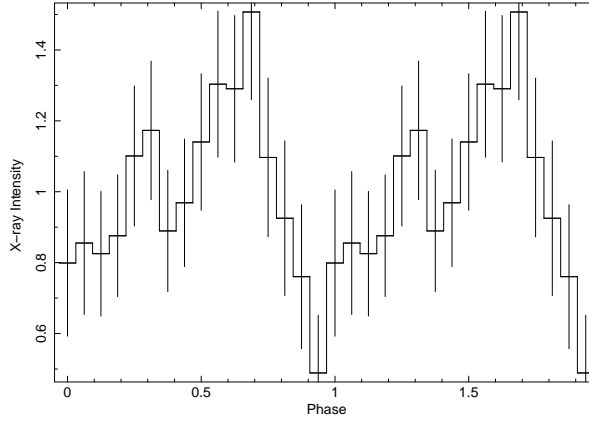


**Figure 7:** X-ray data of V2069 Cyg folded on the 743.385 s spin cycle (16 bins/period). Reference time  $T_0$  set at 55014.000 MJD. Energy range 0.3-10 keV.

material which might have lower opacity in the vertical direction, thus preferentially beaming X-rays along magnetic field lines. The two magnetic poles would combine to produce a double-peaked pulsation [9].

In addition we adopted Mukai's classification (<http://asd.gsfc.nasa.gov/Koji.Mukai/iphone/iphone.html>) of IPs and updated his  $P_{\text{spin}}-P_{\text{orb}}$  diagram including V2069 Cyg which is shown in the Fig. 8 and Tab. 2. Several IPs are found close to  $P_{\text{spin}} / P_{\text{orb}} = 0.1$ . There are 25 systems in the range  $0.01 < P_{\text{spin}} / P_{\text{orb}} < 0.25$  and  $P_{\text{orb}} > 3$  hrs, 4 systems with  $P_{\text{spin}} / P_{\text{orb}} \geq 0.1$  and  $P_{\text{orb}} < 2$  hrs, and only one system with  $P_{\text{spin}} / P_{\text{orb}} \sim 0.049$  that lies in the 'period gap'. Finally there are 5 systems with  $P_{\text{spin}} / P_{\text{orb}} < 0.01$ . Those are defined as fast rotating white dwarfs. Only one of them shows propeller behavior, i.e. AE Aqr. They also show the soft X-ray blackbody

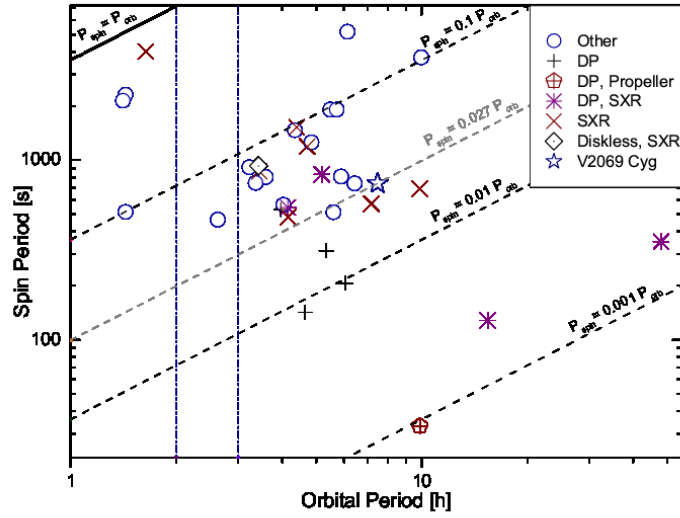


**Figure 8:**  $P_{\text{orb}}-P_{\text{spin}}$  diagram of 35 IPs: DP - double-peak pulsation; SXR - soft X-ray component; diskless - have no accretion disk. The vertical dashed lines show the approximate location of the ‘period gap’, and the diagonal lines are for  $P_{\text{spin}}=P_{\text{orb}}$  (solid) and  $P_{\text{spin}} = 10/100/100 \times P_{\text{orb}}$  (dashed). V2069 Cyg is located well within the population of double peak IPs with soft X-ray component but has a rather low spin-orbit period ratio of 0.0276.

component in their spectrum [10, 11, 12, 13, 14].

#### 4. Conclusions

We conclude that V2069 Cyg is an example of an intermediate polar that shows the double-peak pulsations. It shows a soft blackbody component in X-ray spectrum and its soft X-ray and optical emission have a double-peaked modulation likely associated with the white dwarf spin period. We have also performed the simultaneous optical/X-ray observations of V2069 Cyg to search for any delays between these two energy bands. These data are being analyzed. In the near future we will also perform polarization observations of this system to better constrain its geometry.

#### Acknowledgments

A. Słowikowska acknowledges support from the grant N203 387737 of the Polish Ministry of Science and Higher Education, as well as the grant FNP HOM/2009/11B and the EU grant PERG05-GA-2009-249168. I. Nasiroglu acknowledges support from the EU FP6 Transfer of Knowledge Project "Astrophysics of Neutron Stars" (MKTD-CT-2006-042722). G. Kanbach acknowledges support from the EU FP6 Transfer of Knowledge Project ASTROCENTER (MTKD-CT-2006-039965) and the kind hospitality of the Skinakas team at UoC. We thank Arne Rau for discussions on this paper.

#### References

- [1] Cropper M., 1990, *SSRv*, 54, 195

**Table 2:** 35 IPs with known spin and orbital periods, SXR: soft X-ray blackbody components; DP: double-peaked pulse profiles

Name	$P_{\text{orb}}$ (h)	$P_{\text{spin}}$ (s)	$P_{\text{spin}} / P_{\text{orb}}$	Properties	Period Reference
<i><math>0.01 &lt; P_{\text{spin}} / P_{\text{orb}} &lt; 0.25</math> and <math>P_{\text{orb}} &gt; 3</math> hrs</i>					
V709 Cas	5.341	312.780	0.01627	DP	[17, 43]
NY Lup	9.870	693.010	0.01950	SXR	[14, 30, 12]
RXS J213344.1+510725	7.190	570.820	0.02205	SXR	[14, 18]
Swift J0732.5-1331	5.604	512.420	0.02540	-	[46, 51]
V2069 Cyg	7.480	742.384	0.02756	SXR, DP	[7, 6]
RXS J070407.9-262501	4.167	480.708	0.03204	SXR	[14, 32]
El Uma	6.430	741.660	0.03204	-	[16, 50]
V405 Aur	4.160	545.456	0.03642	SXR, DP	[14, 9, 33]
YY Dra	3.969	529.310	0.03705	DP	[34, 43]
IGR J15094-6649	5.890	809.700	0.03819	-	[25]
IGR J00234+6141	4.033	563.500	0.03881	-	[19]
PQ Gem	5.190	833.400	0.04461	SXR, DP	[31, 12, 37]
V1223 Sgr	3.366	745.630	0.06153	-	[24, 49]
AO Psc	3.591	805.200	0.06229	-	[49]
UU Col	3.450	863.500	0.06952	SXR	[14, 22, 12]
MU Cam	4.719	1187.250	0.06989	SXR	[14, 48]
FO Aqr	4.850	1254.400	0.07184	-	[29]
V2400 Oph	3.430	927.660	0.07513	SXR, Diskless	[14, 21, 36]
BG Cmi	3.230	913.000	0.07852	-	[28]
TX Col	5.718	1911.000	0.09284	-	[52]
V2306 Cyg	4.350	1466.600	0.09365	-	[44]
RXS J180340.0-401214	4.402	1520.510	0.09595	SXR	[14, 32]
TV Col	5.486	1911.000	0.09676	-	[35, 53]
V1062 Tau	9.952	3726.000	0.10400	-	[40]
V1425 Aql	6.139	5188.300	0.23476	-	[47]
<i><math>P_{\text{spin}} / P_{\text{orb}} \geq 0.1</math> and <math>P_{\text{orb}} &lt; 2</math> hrs</i>					
HT Cam	1.433	515.0592	0.09984	-	[41]
V1025 Cen	1.410	2147.000	0.42297	-	[39]
DW Cnc	1.435	2314.660	0.44806	-	[45]
EX Hya	1.637	4021.000	0.68231	SXR	[15, 14, 12]
<i>Period Gap (<math>2</math> hrs <math>&lt; P_{\text{orb}} &lt; 3</math> hrs)</i>					
XSS J00564+4548	2.624	465.680	0.04929	-	[20, 23]
<i>Fast rotator (<math>P_{\text{orb}} / P_{\text{spin}} &lt; 0.01</math>)</i>					
AE Aqr	9.880	33.076	0.00093	DP, Propeller	[26, 36, 43]
GK Per	47.923	351.332	0.00204	SXR, DP	[27, 12, 42, 43]
IGR J17303-0601	15.420	128.000	0.00231	SXR, DP	[14, 24]
DQ Her	4.650	142.000	0.00848	DP	[43, 54]
XY Ari	6.065	206.300	0.00945	DP	[38, 43]

- [2] Patterson J., 1994, *PASP*, 106, 209
- [3] Warner B., 1995, cvs..book
- [4] Hellier C., 2001, cvs..book
- [5] Motch C., Haberl F., Guillout P., Pakull M., Reinsch K., Krautter J., 1996, *A&A*, 307, 459
- [6] Thorstensen J. R., Taylor C. J., 2001, *MNRAS*, 326, 1235
- [7] de Martino D., Bonnet-Bidaud J. M., Falanga M., Mouchet M., Motch C., 2009, *ATel*, 2089, 1
- [8] Kanbach G., Kellner S., Schrey F. Z., Steinle H., Straubmeier C., Spruit H. C., 2003, *SPIE*, 4841, 82
- [9] Evans P. A., Hellier C., 2004, *MNRAS*, 353, 447
- [10] Norton A. J., Somerscales R. V., Wynn G. A., 2004, *ASPC*, 315, 216
- [11] Parker T. L., Norton A. J., Mukai K., 2005, *A&A*, 439, 213
- [12] Evans P. A., Hellier C., 2007, *ApJ*, 663, 1277
- [13] Norton A. J., Mukai K., 2007, *A&A*, 472, 225
- [14] Anzolin G., de Martino D., Bonnet-Bidaud J.-M., Mouchet M., Gänsicke B. T., Matt G., Mukai K., 2008, *A&A*, 489, 1243
- [15] Allan A., Hellier C., Beardmore A., 1998, *MNRAS*, 295, 167
- [16] Baskill D. S., Wheatley P. J., Osborne J. P., 2005, *MNRAS*, 357, 626
- [17] Bonnet-Bidaud J. M., Mouchet M., de Martino D., Matt G., Motch C., 2001, *A&A*, 374, 1003
- [18] Bonnet-Bidaud J. M., Mouchet M., de Martino D., Silvotti R., Motch C., 2006, *A&A*, 445, 1037
- [19] Bonnet-Bidaud J. M., de Martino D., Falanga M., Mouchet M., Masetti N., 2007, *A&A*, 473, 185
- [20] Bonnet-Bidaud J. M., de Martino D., Mouchet M., 2009, *ATel*, 1895, 1
- [21] Buckley D. A. H., Sekiguchi K., Motch C., O'Donoghue D., Chen A.-L., Schwarzenberg-Czerny A., Pietsch W., Harrop-Allin M. K., 1995, *MNRAS*, 275, 1028
- [22] Burwitz V., Reinsch K., Beuermann K., Thomas H.-C., 1996, *A&A*, 310, L25
- [23] Butters O. W., Norton A. J., Hakala P., Mukai K., Barlow E. J., 2008, *A&A*, 487, 271
- [24] Butters O. W., Katajainen S., Norton A. J., Lehto H. J., Piirola V., 2009, *A&A*, 496, 891
- [25] Butters O. W., Norton A. J., Mukai K., Barlow E. J., 2009, *A&A*, 498, L17
- [26] Choi C.-S., Dotani T., Agrawal P. C., 1999, *ApJ*, 525, 399
- [27] Crampton D., Fisher W. A., Cowley A. P., 1986, *ApJ*, 300, 788
- [28] de Martino D., Mouchet M., Bonnet-Bidaud J. M., Vio R., Rosen S. R., Mukai K., Augusteijn T., Garlick M. A., 1995, *A&A*, 298, 849
- [29] de Martino D., Silvotti R., Buckley D. A. H., Gänsicke B. T., Mouchet M., Mukai K., Rosen S. R., 1999, *A&A*, 350, 517
- [30] de Martino D., Bonnet-Bidaud J.-M., Mouchet M., Gänsicke B. T., Haberl F., Motch C., 2006, *A&A*, 449, 1151
- [31] Duck S. R., Rosen S. R., Ponman T. J., Norton A. J., Watson M. G., Mason K. O., 1994, *MNRAS*, 271, 372

- [32] Gänsicke B. T., et al., 2005, MNRAS, 361, 141
- [33] Harlaftis E. T., Horne K., 1999, MNRAS, 305, 437
- [34] Haswell C. A., Patterson J., Thorstensen J. R., Hellier C., Skillman D. R., 1997, ApJ, 476, 847
- [35] Hellier C., 1993, MNRAS, 264, 132
- [36] Hellier C., 2007, IAUS, 243, 325
- [37] Hellier C., Ramseyer T. F., Jablonski F. J., 1994, MNRAS, 271, L25
- [38] Hellier C., Mukai K., Beardmore A. P., 1997, MNRAS, 292, 397
- [39] Hellier C., Wynn G. A., Buckley D. A. H., 2002, MNRAS, 333, 84
- [40] Hellier C., Beardmore A. P., Mukai K., 2002, A&A, 389, 904
- [41] Kemp J., Patterson J., Thorstensen J. R., Fried R. E., Skillman D. R., Billings G., 2002, PASP, 114, 623
- [42] Mauche C. W., 2004, ASPC, 315, 120
- [43] Norton A. J., Beardmore A. P., Allan A., Hellier C., 1999, A&A, 347, 203
- [44] Norton A. J., Quaintrell H., Katajainen S., Lehto H. J., Mukai K., Negueruela I., 2002, A&A, 384, 195
- [45] Patterson J., et al., 2004, PASP, 116, 516
- [46] Patterson J., Halpern J., Mirabal N., Christie G., McCormick J., Rea R., Messier D., 2006, ATel, 757, 1
- [47] Retter A., Leibowitz E. M., Kovo-Kariti O., 1998, MNRAS, 293, 145
- [48] Staude A., Schwöpe A. D., Krumpke M., Hambaryan V., Schwarz R., 2003, A&A, 406, 253
- [49] Taylor P., Beardmore A. P., Norton A. J., Osborne J. P., Watson M. G., 1997, MNRAS, 289, 349
- [50] Thorstensen J. R., 1986, AJ, 91, 940
- [51] Thorstensen J. R., Patterson J., Halpern J., Mirabal N., 2006, ATel, 767, 1
- [52] Tuohy I. R., Buckley D. A. H., Remillard R. A., Bradt H. V., Schwartz D. A., 1986, ApJ, 311, 275
- [53] Vrtilik S. D., Silber A., Primini F., Raymond J. C., 1996, ApJ, 465, 951
- [54] Zhang E., Robinson E. L., Stiening R. F., Horne K., 1995, ApJ, 454, 447